

Simplify Your Multiomics Workflow

Pre-Optimized Antibody Cocktails for Mouse and Human Targets



Presentation of Cryptic Peptides by MHC Class I Is Enhanced by Inflammatory Stimuli

Sharanya Prasad, Shelley R. Starck and Nilabh Shastri

This information is current as of March 11, 2022.

J Immunol 2016; 197:2981-2991; Prepublished online 19 September 2016;

doi: 10.4049/jimmunol.1502045

<http://www.jimmunol.org/content/197/8/2981>

Supplementary Material <http://www.jimmunol.org/content/suppl/2016/09/17/jimmunol.1502045.DCSupplemental>

References This article **cites 40 articles**, 19 of which you can access for free at: <http://www.jimmunol.org/content/197/8/2981.full#ref-list-1>

Why *The JI*? Submit online.

- **Rapid Reviews! 30 days*** from submission to initial decision
- **No Triage!** Every submission reviewed by practicing scientists
- **Fast Publication!** 4 weeks from acceptance to publication

**average*

Subscription Information about subscribing to *The Journal of Immunology* is online at: <http://jimmunol.org/subscription>

Permissions Submit copyright permission requests at: <http://www.aai.org/About/Publications/JI/copyright.html>

Email Alerts Receive free email-alerts when new articles cite this article. Sign up at: <http://jimmunol.org/alerts>



Presentation of Cryptic Peptides by MHC Class I Is Enhanced by Inflammatory Stimuli

Sharanya Prasad, Shelley R. Starck, and Nilabh Shastri

Cytolytic T cells eliminate infected or cancer cells by recognizing peptides presented by MHC class I molecules on the cell surface. The antigenic peptides are derived primarily from newly synthesized proteins including those produced by cryptic translation mechanisms. Previous studies have shown that cryptic translation can be initiated by distinct mechanisms at non-AUG codons in addition to conventional translation initiated at the canonical AUG start codon. In this study, we show that presentation of endogenously translated cryptic peptides is enhanced by TLR signaling pathways involved in pathogen recognition as well as by infection with different viruses. This enhancement of cryptic peptides was caused by proinflammatory cytokines, secreted in response to microbial infection. Furthermore, blocking these cytokines abrogated the enhancement of cryptic peptide presentation in response to infection. Thus, presentation of cryptic peptides is selectively enhanced during inflammation and infection, which could allow the immune system to detect intracellular pathogens that might otherwise escape detection because of inhibition of conventional host translation mechanisms. *The Journal of Immunology*, 2016, 197: 2981–2991.

On the cell surface, a diverse set of peptides is presented by MHC class I (MHC I) molecules (1–3). Cytotoxic CD8⁺ T cells of the immune system can bind these peptide-MHC complexes and trigger an immune response by recognizing non-self-antigenic peptides. Peptides that are presented on MHC I molecules to CD8⁺ T cells are derived mostly from endogenous sources—degradation of endogenously synthesized proteins or newly synthesized proteins. Apart from some viral proteins that are resistant to degradation, all endogenously synthesized proteins contribute to the antigenic peptide repertoire (3). This peptide repertoire is known to arise largely from newly synthesized proteins, which allows early viral proteins to be detected regardless of their stability (4). In addition, proteins undergoing turnover would also contribute to the peptide display (5). The newly synthesized polypeptides that are targeted for degradation are known as defective ribosomal products or DRiPs, which are known to couple protein synthesis to the MHC I presentation pathway (6). Some of the endogenously generated peptides in the MHC I pathway can also originate from sources other than translation of the primary open reading frame. These sources are

termed cryptic because their origin was unknown (7). The cryptic antigenic peptides contribute to the diversity of the peptide repertoire presented on the cell surface making the process of immune surveillance more effective.

Cryptically translated antigenic peptides can arise from several different sources. Some of these sources include alternative reading frames (ARFs) of an mRNA transcript (3, 8), read-through of stop codons into the 3'-untranslated region (9) and ribosomal frame-shifting (10, 11). Yet another source from which cryptic peptides arise is the use of a non-AUG initiation codon to initiate protein translation (12, 13).

Cryptic translation of either viral or endogenous mRNAs can give rise to cryptic peptide MHC (pMHC) (14). Cryptic peptides arising from the ARFs of HIV and other retroviral ARFs and their role in protective immunity have been well characterized (15, 16). Some of these T cell responses to cryptic peptides arising from HIV were shown to be necessary to control viral load in human HIV-infected patients (17). Furthermore, cryptic peptides arising from adenoviral vectors, used in a gene therapy trial, were also shown to elicit abnormal T cell responses (18). In addition to virally induced cryptic peptides, there are several examples of cryptic peptides arising from endogenous sources. T cell responses to cryptic epitopes arising from proteins AIM2 and NA17-A in melanoma patients were shown to be used for immune monitoring (19). Furthermore, cryptic CD8⁺ T cell epitopes from the VEGF gene were shown to arise through alternative initiation from a CUG codon (20). Given that all cell types are capable of presenting cryptic peptides (21) suggests that cryptic translation is a widespread phenomenon.

Since its initial discovery, the mechanism of CUG-initiated translation has been shown to be distinct from conventional AUG-initiated translation. A subset of ribosomes scans specifically for an alternate CUG initiation codon, which was unexpectedly found to be decoded as leucine rather than the canonical methionine residue (12, 13, 21). Furthermore, a novel initiator, transfer RNA (tRNA), was found to be present at CUG initiation codons, which decoded CUG as a leucine (22). Perhaps because of the distinct mechanism, CUG-initiated translation was found to be resistant to several compounds that inhibited initiation at canonical AUG codons (23). This led to the question of, if other cellular

Division of Immunology and Pathogenesis, Department of Molecular and Cell Biology, University of California, Berkeley, Berkeley, CA 94720

ORCID: 0000-0002-7021-3664 (S.P.); 0000-0001-6231-9082 (S.R.S.).

Received for publication September 17, 2015. Accepted for publication August 16, 2016.

This work was supported by grants from the National Institutes of Health (to N.S.). S.R.S. was supported in part by a National Institutes of Health training grant, a postdoctoral fellowship from the Cancer Research Institute, and a National Research Service Award Fellowship from the National Institutes of Health.

S.P. and N.S. designed the study; S.P. and S.R.S. carried out the experiments and analyzed the data; and S.P. and N.S. wrote the manuscript.

Address correspondence and reprint requests to Dr. Nilabh Shastri, Division of Immunology and Pathogenesis, Department of Molecular and Cell Biology, University of California, Berkeley, Berkeley, CA 94720-3200. E-mail address: nshastri@berkeley.edu

The online version of this article contains supplemental material.

Abbreviations used in this article: ARF, alternative reading frame; CPRG, chlorophenol red-β-D-galactopyranoside; MCMV, mouse CMV; MHC I, MHC class I; MOI, multiplicity of infection; pMHC, peptide MHC; tRNA, transfer RNA; UPR, unfolded protein response.

Copyright © 2016 by The American Association of Immunologists, Inc. 0022-1767/16/\$30.00

stresses some of which inhibit conventional translation, could regulate presentation of cryptic peptides.

In this study, we used *in vitro* as well as *ex vivo* model systems to study whether presentation of cryptic peptides was regulated by physiological stimuli. We found that T cell responses to the cryptic CUG-initiated peptide were enhanced during viral infections and other inflammatory conditions. This enhancement in presentation of cryptic peptides was mediated by inflammatory cytokines.

Materials and Methods

Mice, cell lines, and reagents

W19.LYL8 transgenic mice have been described elsewhere (21). C57BL/6J and B10.D2 mice were purchased from The Jackson Laboratory (Bar Harbor, ME). All mouse work was done with the approval of the Animal Care and Use Committee of the University of California (Berkeley, CA). K^b expressing L, Cos7, and BCZ103 cell lines have been described before (24, 25), and 11p9Z (26), 30NXZ (27), NIH3T3, and BALB 3T3 cells were obtained from American Tissue Culture Collection (Manassas, VA). C57BL/6J immortalized-macrophages were a gift from the laboratory of Prof. G. Barton (University of California, Berkeley, CA). M-CSF-producing cells (3T3-MCSF) were a gift from the laboratory of Prof. R. Vance (University of California, Berkeley, CA). TLR agonists were obtained from InvivoGen.

Generation of primary W19.LYL8 bone marrow macrophages

Legs were dissected from W19.LYL8 mice, and the femur and tibia were cleaned off from the surrounding muscle tissue and cleaned in 70% ethanol. The bones were cut, and the marrows were flushed using a 24 1/2-gauge needle into complete RPMI 1640 with 10% FBS. The suspended marrows were then filtered through a 0.4- μ m mesh filter. The bone marrow cells were resuspended in 1 ml of RBC lysis buffer for 1 min and washed with complete RPMI 1640 medium. Cells were then counted and plated into sterile petri dishes at 5–6 million cells per dish in special medium with 20% FBS and 20% M-CSF.

mRNA transfection

mRNA was generated using the mMessage mMachine T7 Transcription kit (Ambion). Plasmid DNA was linearized with HpaI and used as templates for transcription by T7 RNA polymerase (mMessage mMachine T7; Ambion). Transcription reactions contained m7GTP or ARCA m7GTP cap analog (Ambion) to yield naturally capped mRNAs. The Poly(A) Tailing Kit (Ambion) was used to add poly(A) tails onto mRNAs. Transcribed mRNAs were purified using phenol:CHCl₃ according to the manufacturer's recommendation followed by purification using illustra MicroSpin G-25 columns (GE Healthcare Life Sciences). *In vitro*-transcribed mRNAs were stored in water at -80°C . The TransMessenger Transfection Reagent (Qiagen) was used for transfection of mRNA into cells. For each microgram of mRNA, a mix of 16.5 μ l of Enhancer and up to 100 μ l of buffer EC was made and incubated for 5 min at room temperature. Thirty-three microliters of TransMessenger Reagent was added and incubated for 10 min at room temperature. A total of 900 μ l of serum-free medium was added to the mix and added on to the cells. After 4 h, medium on cells was replaced with complete RPMI 1640 with or without various TLR agonists.

T cell hybridoma assays

T cell hybrids are LacZ inducible, and LacZ activity is measured in the T cell hybridoma assays. After coculture of APCs and T cell hybridoma cells for 18 h in a 96-well flat-bottom plate, 100 μ l of chlorophenol red- β -D-galactopyranoside (CPRG; purchased from Roche Diagnostics) solution is added to each well. Absorbance was measured at dual wavelengths 595 and 655 nm as reference.

HPLC fractionation assay

Cos7 cells (150,000–250,000 cells per well of 6-well plate) were transfected with the different [ATG]-YL8 or [CTG]-YL8, TLR 2, and K^b constructs and thereafter stimulated with Pam₃CSK₄. Transfected cells were resuspended in 10% acetic acid and boiled at 100°C for 10 min. The boiled suspension of cells was then spun down at 10,000 rpm for 15 min. The supernatant was transferred to a 10-kDa Millipore filter (Ambion) and spun down at 13,000 rpm for 45 min. The flow-through was injected into a C18 column and separated by reversed-phase HPLC. A program with a ratio of 80% buffer A (0.1% trifluoro acetic acid in water) and 20% buffer B (0.1% trifluoro acetic acid in acetonitrile) was used. Three-drop fractions were collected in a flat-bottom 96-well plate. The plates were

dried by spinning overnight in a vacuum-trap-based plate dryer. The following day, 50,000 K^b-L cells and 100,000 BCZ103 hybridoma were added to each well of the 96-well plate. The antigenic peptide activity was detected and quantified by the T cell activation assay described above.

Virus infection

Mouse CMV (MCMV) (Smith strain) and influenza virus (strains WSN33 and PR8) were obtained from the laboratory of Prof. L. Coscoy (University of California, Berkeley, CA). For both infections, 1 million bone marrow macrophages were plated into each well of a 6-well plate. The next day, the medium on the cells was removed and stored in a 50-ml tube as conditioned medium. One milliliter of viral supernatant (at multiplicity of infection [MOI] of 0.5–1.0) or complete RPMI medium was added to the cells for 2 h. This was then removed and replaced with 1 ml of fresh medium and 1 ml of the conditioned medium. After 6 h, the macrophages were harvested with cold PBS with 1 mM EDTA and scraped off the plate using cell lifters. Cells were resuspended in complete RPMI 1640 and a T cell assay was set up.

Virus preparation

One million NIH3T3 cells were plated into a T75 flask on the previous night in 10 ml of complete DMEM. Medium on the cells was replaced with DMEM complete medium + MCMV virus at an MOI of 0.1, in a total volume of 4 ml, for 2 h. Six milliliters of complete DMEM was added thereafter, and the cells were observed for 4 d. Once a beaded formation of cells began to form, the supernatant from the cells was harvested the next day. To harvest the virus, supernatant from the cells was spun down at 1200 rpm for 5 min. Supernatant was then filtered through a 0.45- μ m filter and stored at -80°C .

Plaque assay

A total of 150,000 BALB 3T3 cells were plated into each well of a 6-well plate. Serial dilutions of virus were made in complete DMEM. Serial dilutions of 1:10, 1:100, 1:1,000, and 1:10,000 were made by adding 300 μ l of virus into 2.7 ml of complete DMEM. One milliliter of the dilution was added into each well and was incubated for 2 h. After 2 h, the supernatant was aspirated, and a mixture of low-melting agarose, MEM + serum, antibiotic, and 40% glucose was added to the cells. On the fifth day, plaques were fixed by adding 10% formaldehyde and visualized by removing agarose and adding crystal violet.

TNF intracellular staining assay

Brefeldin A (GolgiPlug) was added to the treatment condition after 2 h of treatment initiation and left in solution for 4–6 h. Cells were then harvested in FACS buffer and stained for surface MHC I expression. Primary macrophages were treated with FcBlock at a 1:200 concentration in a final volume of 50 μ l for 30 min. Cells were then fixed and permeabilized using CytoFix/CytoPerm solution (100 μ l per well) for 20 min. Cells were then washed with 1 \times perm/wash buffer and incubated with anti-TNF Ab (anti-mouse TNF- α -PE, clone MP6-XT22; eBioscience) or an isotype control Ab (Isotype-PE conjugated, rat IgG1, clone eBRG1; eBioscience) at a concentration of 1:100 in a final volume of 50 μ l for 30 min–1 h. Cells were then analyzed on the FC-500.

Coculture assays with B10.D2 cells

Primary macrophages were prepared from B10.D2 mice, which have the MHC-H2^D haplotype. B10.D2 macrophages were first infected with MCMV for 6 h. Cells were then harvested, washed, and titrated into a 96-well plate or split into a 96-well plate. B6WT primary macrophages were then added to these cells for 6 h. The supernatant was removed, 100,000 BCZ103 cells were added to the mixture of B10.D2 cells and BCZ103 cells, and a T cell assay was performed.

UV-inactivated virus

MCMV-GFP (obtained from the laboratory of Prof. L. Coscoy) was exposed to UV light inside a sterile hood for 30 min. Cells were infected with this supernatant, and GFP expression was then tested in these cells by flow cytometry. Supernatant that was exposed to UV did not exhibit any GFP expression in the cells, whereas wild-type MCMV-GFP exhibited GFP production in the cells. Inactivation was also tested by a plaque assay. UV-inactivated MCMV did not produce any plaques in the diluted samples.

TNF and IFNAR-blocking experiments

Primary macrophages were infected with MCMV or left untreated and treated with anti-TNF- α Ab (mouse TNF- α Ab, monoclonal rat IgG1,

clone MP6-XT22; R&D Systems) or an isotype control Ab (Rat IgG1 isotype control, monoclonal rat IgG1, clone 43414; R&D Systems) for 6 h. For IFNAR blocking, an anti-IFNAR-1 Ab (LEAF purified anti-mouse IFNAR-1, clone MAR1-5A3; BioLegend) or Isotype control (LEAF purified mouse IgG1 κ isotype control, clone MG1-45; BioLegend) was used. Cells were harvested and T cell assay was performed. The Abs (blocking or isotype control) were included during the incubation with T cells. During the incubation with T cells, anti-TNF- α or isotype Ab was included.

Luciferase assays with L929-ISRE cells

Supernatant from uninfected and infected cells were added to L929-ISRE cells (obtained from Dr. A. Winoto's laboratory, University of California, Berkeley, CA). These cells were then lysed using the reagents of the Promega Luciferase assay. Luciferin reagent was then added to the lysed cells, and the absorbance was measured.

Results

Model system to study cryptic translation of antigenic peptides

We examined the presentation of cryptic pMHC I using cDNA constructs encoding either the LYL8 (LTFNYRNL) peptide or its analog MYL8 (MTFNYRNL) as a model (Fig. 1, top panel). These two constructs differ only in the first amino acid encoded by either the CUG (cryptic) or AUG (conventional) initiation codon. Cells transfected with these constructs decode their CUG or AUG initiation codons as Leu and Met, respectively, by either cryptic or canonical translation (13). An important feature of these constructs is that a CUG start codon can be decoded into a Met amino acid by wobble base pairing. Therefore, the construct starting with a CUG gives rise to a combination of MYL8 and LYL8 peptides (13, 23). To obviate transcription and posttranscriptional regulation, mRNA generated from these cDNAs encoding LYL8 or MYL8 were transfected into macrophages, followed by TLR agonist stimulation. The presentation of translated peptides was measured with the BCZ103 T cell hybridoma, which responds to either the LYL8 or the MYL8 peptides bound to the K^b MHC I molecule (12). Upon activation, the BCZ103 hybridoma produces the reporter lacZ that is measured by the conversion of the CPRG substrate to a red product by its absorbance at 595 nm. Therefore, Ag presentation and T cell activation is used as a read out for the translation levels of these peptides in the cell.

In addition to this *in vitro* assay, we also used primary cells from a transgenic mouse model, which expresses a bicistronic transgene WI9.LYL8, were obtained (Fig. 1, bottom panel) (21). This transgene enables identification of naturally processed peptides that are generated in the conventional versus cryptic context. The transgene encodes two peptides; the first one is a WI9 peptide

derived from the Y-chromosome gene *Uty*, placed in a conventional AUG initiated translational context. The second peptide, LYL8, was placed in a cryptic translational context, downstream of the stop codon with CUG as the initiation codon. In this model system, however, the CUG start codon is decoded only as a leucine and gives rise to the LYL8 peptide exclusively (21). Therefore, this transgenic model allows study of conventional and cryptic translation from the same gene. The WI9 peptide is presented on the D^b MHC I molecule and is detected by the lac Z-inducible, 11p9Z T cell hybridoma, whereas the LYL8 peptide, as described above, is presented on the K^b MHC I molecule and detected by the BCZ103 T cell hybridoma.

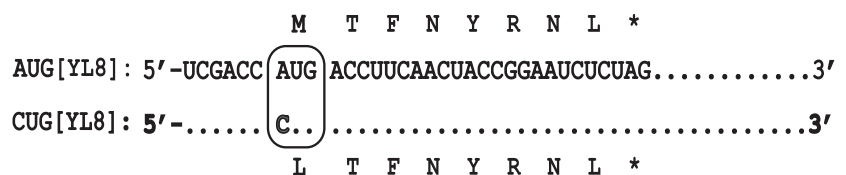
TLR agonists enhance presentation of cryptic pMHC I

When the mRNA generated from these constructs were transfected into macrophages, followed by treatment with Pam₃CSK₄ (a bacterial lipoprotein) a TLR2 agonist, the T cell response to the CUG-initiated peptide, LYL8, was enhanced, compared with the untreated sample (Fig. 2A). In contrast, the T cell response to cells transfected with the AUG-initiated peptide MYL8 was not altered by the Pam₃CSK treatment. Note that cells transfected with mRNAs of the control construct [CCC]-YL8 did not yield detectable pMHC I because [CCC] is not an effective initiation codon. A similar enhancement in Ag presentation was observed when transfected cells were treated with CpG (unmethylated CpG nucleotides) a TLR9 agonist was used (Fig. 2B). To establish statistical significance, T cell responses to the AUG-YL8 and CUG-YL8 peptide, upon Pam₃CSK₄ and CpG stimulation, were normalized to that of the untreated cells, averaged across three distinct experiments and plotted as a line graph. The trend of each line indicates the effect of the condition (Fig. 2C). T cell responses to the cryptic peptide are significantly enhanced compared with that of the conventional peptide, for which the T cell responses tend to diminish upon TLR ligand stimulation.

In addition to using immortalized cell lines in the *in vitro* model system, we used primary cells isolated from the WI9.LYL8 transgenic mice to extend these observations to normal cells. Bone marrow-derived macrophages were generated from these transgenic mice, and the macrophages were stimulated with these various agonists such as Pam₃CSK₄, CpG, and LPS. Cells treated with each agonist enhanced the cryptic peptide-specific T cell response robustly, compared with the untreated cells. In contrast, the 11p9Z T cell response against the AUG-initiated WI9 peptide remained unchanged with or without agonist treatment (Fig. 2D). To establish statistical significance, T cell responses to

FIGURE 1. Model systems to study cryptic translation. **(A)** mRNA sequences encoding the MYL8 or [AUG]-YL8 and the LYL8 or [CUG]-YL8 peptides are shown. The sequences differ only at a single nucleotide (A > C) within the boxed initiation codon. **(B)** Bicistronic transgene encoding the WI9 and LYL8 peptides. The conventional [AUG] initiated WI9 is followed by a stop codon and the cryptic [CUG] initiated LYL8 peptide.

A *In-vitro* model



B *Ex-vivo* model

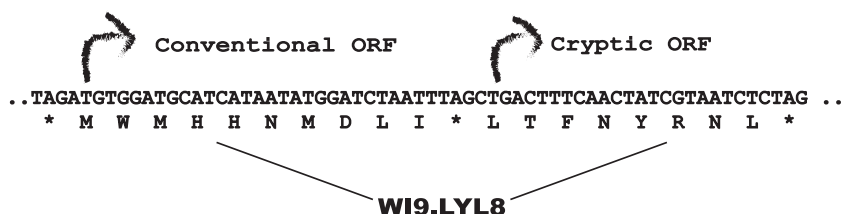




FIGURE 2. TLR agonists enhance cryptic peptide presentation. **(A)** The mRNA encoding MYL8 ([AUG]-YL8) and LY8 ([CUG]-YL8) peptides along with the negative control ([CCC]-YL8) were transfected into wild-type immortalized macrophages. After 3 h, half of the transfected samples were treated with TLR2 agonist Pam₃CSK₄ (1 μg/ml) for 4 h. The macrophages were then harvested and cultured with the lacZ-inducible, BCZ103 T cell hybridoma. The response of BCZ103 T cells, shown on the y-axis, is a measure of the β-galactosidase activity determined by the conversion of the CPRG substrate to a colored product with an absorbance at 595 nm. The cell numbers in each well is indicated on the x-axis. Data are representative of 11 experiments. **(B)** Identical experimental setup as in (A) except TLR9 agonist CpG was used as the agonist. Y-axis indicates the BCZ103 T cell response, and x-axis indicates the cell number per well. Data are representative of eight experiments. **(C)** T cell responses to the AUG-YL8 and CUG-YL8 peptides, upon Pam₃CSK₄ (i) stimulation or CpG stimulation (ii), were normalized to that of the untreated samples for three distinct experiments. An unpaired *t* test (with Welch's correction) was performed, comparing the two variables; *p* < 0.05. **(D)** Primary macrophages were isolated from the W19.LYL8 transgenic mice and stimulated with indicated TLR agonists (1 μg/ml) for 6 h and then cultured with either the T cell hybridoma 11p9Z-specific for the W19 peptide or the LY8-specific BCZ103 hybridoma. Macrophages from wild-type mice were used as a negative control. Y-axis indicates the T cell response (11p9Z-specific hybridoma response for conventional peptide and BCZ103 hybridoma response for the cryptic peptide), and the x-axis indicates the cell number per well.

the WI9 and LYL8 peptide, upon Pam₃CSK₄, CpG, and LPS stimulation, were normalized to that of the untreated cells, averaged across three distinct experiments and plotted as a line graph. T cell responses to TLR-ligand stimulation were significantly enhanced for the LYL8 peptide. T cell responses to the WI9 peptide were not affected in a significant manner, upon TLR-ligand stimulation (Supplemental Fig. 1A). Statistical significance of the enhancement was calculated in a similar way as described for Fig. 2C.

Furthermore, to ensure that this was a direct effect of the TLR agonist stimulation and subsequent activation of signaling pathways in the macrophage, TNF- α production was measured by intracellular cytokine staining and analysis by flow cytometry. All of the TLR agonist stimulations, led to production in macrophages, showing that this was an effect of macrophage activation (Supplemental Fig. 1B).

Therefore, in both the in vitro model system and the ex vivo model systems, we found that different TLR agonists enhanced cryptic peptide presentation substantially more than conventional peptide presentation.

TLR agonist enhanced amounts of naturally processed cryptic peptide

We analyzed the translated peptides directly by fractionating lysates of transfected cells by reversed-phase HPLC. The cDNA constructs transfected into COS 7 cells and antigenic peptides were detected using K^b-expressing L fibroblasts (K89s) as APC and activation of the BCZ103 hybridoma. The T cell response shown on the y-axis to each fraction reflects the relative amount of peptide in each fraction (Fig. 3). In addition, the elution profile of the antigenic activity revealed the structural features of the peptide as established by comparison with synthetic analogs. For both the [AUG]-YL8 and the [CUG]-YL8 constructs, the antigenic activities were found in essentially the same fractions indicating that the same peptides were generated from these constructs. Note that the MYL8 peptide elutes in fractions 25–28 and comparable amounts were generated with or without Pam₃CSK treatment of cells transfected with the [AUG]-YL8 construct (Fig. 3, left panel). In contrast, cells transfected with the [CUG]-YL8 construct produced two distinct antigenic activities. The first peak in fractions 25–28 matches the MYL8 peptide, produced by conventional translation, and the second peak at fraction 34–36 corresponds to the LYL8 peptide that is produced by a cryptic translation mechanism (Fig. 3, right panel). Notably, Pam₃CSK treatment enhanced the recovery of only the LYL8 peptide but did not change the recovered MYL8 peptide. Thus, the observed increase of Ag presentation

activity by TLR agonists can be attributed to an increase in cryptic rather than conventional translation. Moreover, TLR agonist stimulation does not modify the peptide in any manner and therefore as evidenced by the peptides eluting at the same fraction with or without TLR agonist treatment.

Pathogen infection enhances presentation of cryptic peptides

TLR agonists are merely simulators of pathogenic infection. To obtain a more physiological assessment, we tested whether virus infection would affect the presentation of cryptic peptides. First, we used the Influenza virus because it is known to inhibit host protein synthesis (28). The WI9.LYL8 macrophages were infected with influenza (PR8 strain) for a duration of 6 and 24 h. Conventional peptide presentation was mildly enhanced at both of those time points; however, cryptic peptide presentation was significantly enhanced (Fig. 4A). Influenza infection of cells was confirmed using an IFN-dependent luciferase reporter assay.

Next, we used the MCMV, a member of the herpesvirus family. Primary bone marrow-derived macrophages were generated from the WI9.LYL8 transgenic mice. These cells were then infected with MCMV at an MOI of 1.0 for a duration of 6 h. Cells were then harvested, and a T cell assay was performed by culturing the cells with either the BCZ103 or the 11p9Z hybridoma. In the presence of the virus, cryptic peptide presentation was considerably enhanced as indicated by the increased BCZ103 response of the infected samples compared with the uninfected samples (Fig. 4B). In addition, we established that T cell responses to LYL8 peptide were enhanced in a statistically significant manner, in response to MCMV and Influenza infection, compared with the T cell responses to the WI9 peptide (Fig. 4C).

To determine whether the enhanced presentation activity was caused by the virus in particular or by a cell-signaling event, mutant MCMV that were lacking multiple different open-reading frames (obtained from the laboratory of Prof. L. Coscoy) were used to infect the WI9.LYL8 transgenic macrophages. All of the mutants were shown to enhance cryptic peptide presentation and the conventional peptide presentation remained unchanged. Only the mutant that was lacking MHC I inhibitors showed increased peptide presentation for both the conventional and cryptic peptides (Supplemental Fig. 2A). This showed that no single viral gene was responsible for this phenomenon in particular. In this analysis, we also incorporated the T cell responses to an endogenous peptide (Supplemental Fig. 2Aiii), outside of the transgene, as a control, to show that the cryptic peptides are indeed differentially enhanced compared with other conventional or endogenous peptides.

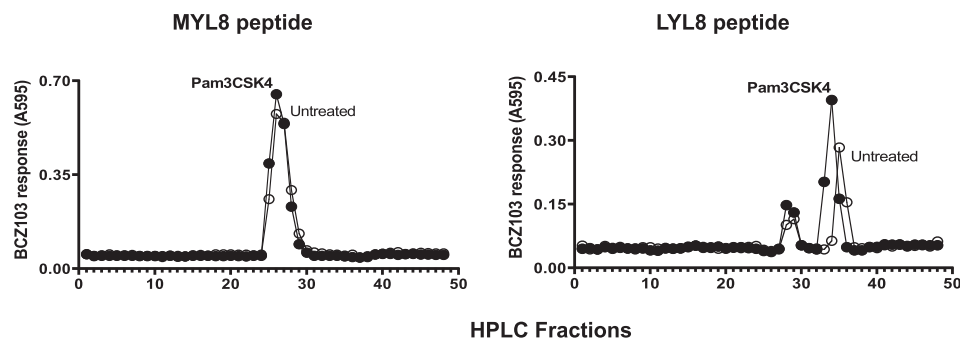


FIGURE 3. TLR agonist enhances amount of cryptic peptide. cDNA constructs encoding [ATG]-YL8 or [CTG]-YL8, along with the K^b MHC I molecule and TLR2, were transfected into Cos7 cells. These cells were then treated with Pam₃CSK₄. Peptides were extracted by acid and fractionated by reversed-phase HPLC. K89 APCs and BCZ103 hybridoma cells were added to the fractionated peptide samples to measure the amount of peptide through the T cell assay. Y-axis indicates the BCZ103 T cell response, and the x-axis indicates the fraction numbers after running the samples through the reversed-phase HPLC. Data are representative of three experiments.

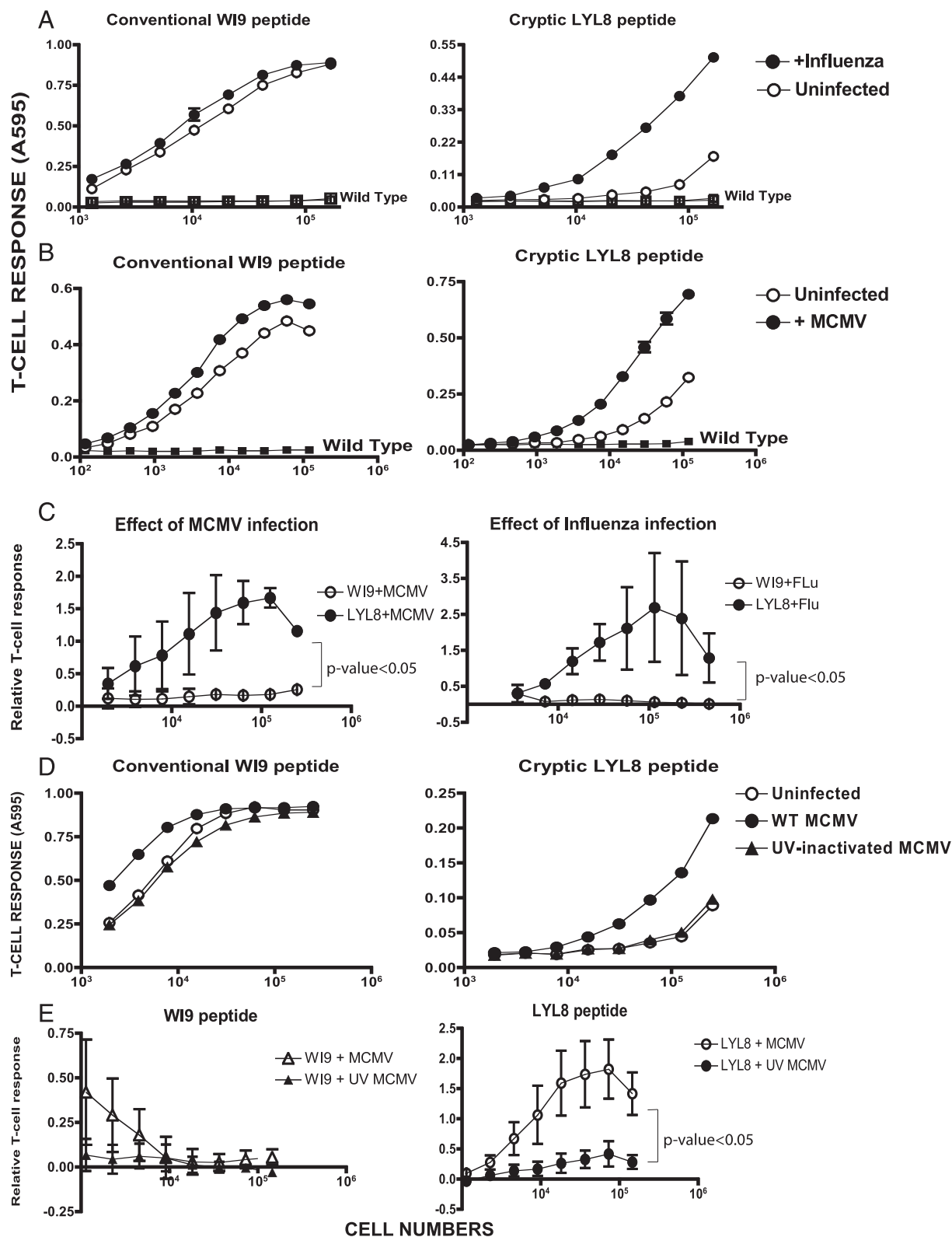


FIGURE 4. Cryptic peptide presentation is enhanced by virus infection. **(A)** Primary macrophages from the WI9.LYL8 transgenic mice were infected with influenza virus at an MOI of 1.0 for 6 h, after which the cells were harvested and assayed for Ag presentation activity using T cell hybridomas as described in Fig. 2D. The y-axis indicates the T cell response (11p9Z hybridoma response for the conventional WI9 peptide and the BCZ103 hybridoma response for the cryptic LYL8 peptide), and x-axis shows the cell numbers per well. Data are representative of three experiments. **(B)** WI9.LYL8 primary macrophages were infected with MCMV at an MOI of 1.0 for 6 h. Cells were then harvested, and a T cell hybridoma assay was set up as described in Fig. 2D. The y-axis indicates the T cell response (11p9Z-specific hybridoma response for the conventional peptide and the BCZ103-specific hybridoma response for the cryptic peptide), and x-axis indicates the cell numbers per well. Data are representative of four experimental repeats. **(C)** T cell responses to the WI9 and LYL8 peptides, upon MCMV infection (left panel) and influenza infection (right panel), were normalized to that of the uninfected samples for three distinct experiments. An unpaired *t* test (with Welch's correction) was performed, comparing the conventional and cryptic peptide responses: $p < 0.05$ **(D)**. WI9.LYL8 macrophages were infected with wild-type MCMV or UV-inactivated MCMV for 6 h. Cells were then harvested (Figure legend continues)

Next, we asked whether virus gene expression was required to cause increase in presentation of cryptic peptides. We tested live versus UV-inactivated MCMV-GFP (MCMV that also had a GFP coding sequence in its genome) for this experiment. The viral supernatant was inactivated by exposure to UV light. The enhancement of cryptic peptide presentation, in this experiment, was 3000-fold in the presence of wild-type MCMV, and there was no enhancement of cryptic peptide presentation in the presence of UV-inactivated MCMV. For conventional peptide presentation, there was only a 4-fold enhancement in the relative T cell response in the presence of wild-type MCMV, whereas relative T cell response was decreased by 30% in the presence of UV-inactivated MCMV (Fig. 4D). This enhancement was calculated by obtaining the number of cells required to establish half-maximal T cell response. This number of cells was then normalized to that of the uninfected condition. This normalized number was compared across wild-type MCMV-treated and UV-inactivated MCMV-treated conditions. This suggested that the live virus was triggering a signaling activity that UV-inactivated virus could not. Moreover, it was expected that UV-inactivated virus would behave like a TLR agonist but that was not the case. The inactivation of the virus was measured by flow cytometry by looking for GFP-positive cells, which were completely absent when UV-inactivated virus was used to infect cells. Furthermore, UV-inactivated virus failed to induce any TNF- α production in an intracellular cytokine-staining assay (Supplemental Fig. 2B). UV-inactivated MCMV has been shown to exhibit reduced inflammatory cytokine production (29). Therefore, it is consistent that we observe decreased TNF- α production when macrophages are infected with UV-inactivated virus. Furthermore, T cell responses to the LYL8 peptide, upon wild-type MCMV virus infection, were enhanced in a statistically significant manner in comparison with UV-inactivated virus infection (Fig. 4E). T cell responses to the WI9 peptide are unchanged upon wild-type MCMV or UV-inactivated virus infection and display an overall decreasing trend.

From these results, we can infer that live pathogen infection enhances presentation of cryptic peptides to T cells, substantially more than presentation of conventional peptides. Moreover, this effect is also greater than what was seen with TLR agonists. Furthermore, UV-inactivated virus was unable to cause the enhancement of cryptic peptides because of the inability of stimulating cytokine production in macrophages.

Enhancement of cryptic peptide presentation does not require direct virus infection

To determine whether the enhanced cryptic peptide presentation was caused directly by live virus infection, a coculture assay was performed. The WI9.LYL8 macrophages are derived from the C57BL/6 strain, which expresses the H-2^b haplotype and the K^b and D^b MHC I molecules. In this experiment, we used primary macrophages of a different haplotype—H-2^d—which express distinct MHC I molecules, K^d, D^d, and L^d, which do not present the WI9 or the LYL8 peptides. We infected the H-2^d macrophages with either wild-type MCMV or UV-inactivated MCMV for 6 h. These H-2^d macrophages were then cocultured with WI9.LYL8 macrophages for a period of 3–6 h. Next, the supernatant from the H-2^d macrophages was filtered through a 0.2- μ M filter to remove

any cells and added to the WI9.LYL8 macrophages. After a duration of 3–6 h, T cell hybridomas were added to the cocultured cells (Fig. 5A). The WI9.LYL8 macrophages that were cocultured with the wild-type MCMV-infected H-2^d macrophages showed enhanced cryptic peptide presentation, whereas those cocultured with the UV-MCMV-infected H-2^d macrophages showed reduced increase in cryptic peptide presentation. Interestingly, when the supernatants were added to the WI9.LYL8 macrophages, the uninfected and uv-inactivated supernatant did not induce measurable enhancement in cryptic peptide presentation, but the wild-type MCMV supernatant showed enhanced cryptic peptide presentation. These results suggest that the APCs do not have to be infected with the virus to show enhanced peptide presentation. Moreover, T cell responses to the LYL8 peptide were significantly enhanced upon wild-type MCMV supernatant stimulation compared with the WI9 peptide (Fig. 5B), which did not show any signs of enhancement. These results suggest that coculture with infected cells was sufficient to induce enhanced cryptic peptide presentation. Moreover, coculture with just the supernatant from infected cells was also sufficient to induce enhanced cryptic peptide presentation. This result implicates soluble factors secreted from infected cells as potential mediators of enhanced Ag presentation activity. This also suggests that the UV-inactivated supernatant might induce very little soluble factors to be secreted into the supernatant, which is why it was unable to induce enhanced cryptic peptide presentation.

To determine whether there was any reinfection of the WI9.LYL8 macrophages, the macrophages were stained with MHC I surface Abs. The H2-D macrophages stained positively for both D^d Ab and MCMV-GFP (Supplemental Fig. 3A). However, the WI9.LYL8 macrophages stained positively only for the D^b Ab and not for MCMV-GFP at all (Supplemental Fig. 3B) ruling out the possibility that the WI9.LYL8 macrophages were infected with residual virus.

To test whether soluble factors, secreted upon viral infection, were responsible for the enhancement of cryptic peptide presentation, we decided to test whether cytokines were able to directly regulate cryptic peptide presentation. We added TNF- α to WI9.LYL8 primary macrophages for 6 h. Cells were then harvested, and a T cell assay was performed. The cells were also treated with the noninflammatory cytokine IL-10. Notably, TNF- α enhanced cryptic peptide presentation by 3-fold, whereas IL-10 did not cause any measurable change in cryptic peptide presentation compared with untreated cells (Fig. 5C). Moreover, conventional peptide presentation was actually decreased by 20% in the presence of these two cytokines, as measured by the relative T cell response. Furthermore, T cell responses to LYL8 peptide were enhanced in a statistically significant manner upon TNF- α stimulation, compared with the IL-10 stimulation, whereas the T cell responses to the WI9 peptide were not significantly affected by either cytokine (Supplemental Fig. 4A, 4B). T cell responses to the LYL8 peptide were also significantly enhanced upon TNF- α stimulation compared with the T cell responses to the WI9 peptide (Supplemental Fig. 4C). Activated macrophages are also known to secrete IFNs upon TLR stimulation. So, we treated primary WI9.LYL8 macrophages with type I and type II IFN. Cryptic, but not conventional peptide presentation was enhanced in the presence of

and a T cell hybridoma assay was set up as described in Fig. 2. The y-axis indicates the T cell response (11p9Z-specific hybridoma response for the conventional peptide and the BCZ103-specific hybridoma response for the cryptic peptide), and x-axis indicates the cell numbers plated. Data are representative of three experiments. (E) T cell responses to the WI9 (left panel) and LYL8 (right panel) peptides upon wild-type and UV-inactivated MCMV infection were normalized to that of the uninfected samples for three distinct experiments. An unpaired *t* test (with Welch's correction) was performed, comparing the wild-type and UV-inactivated T cell responses.

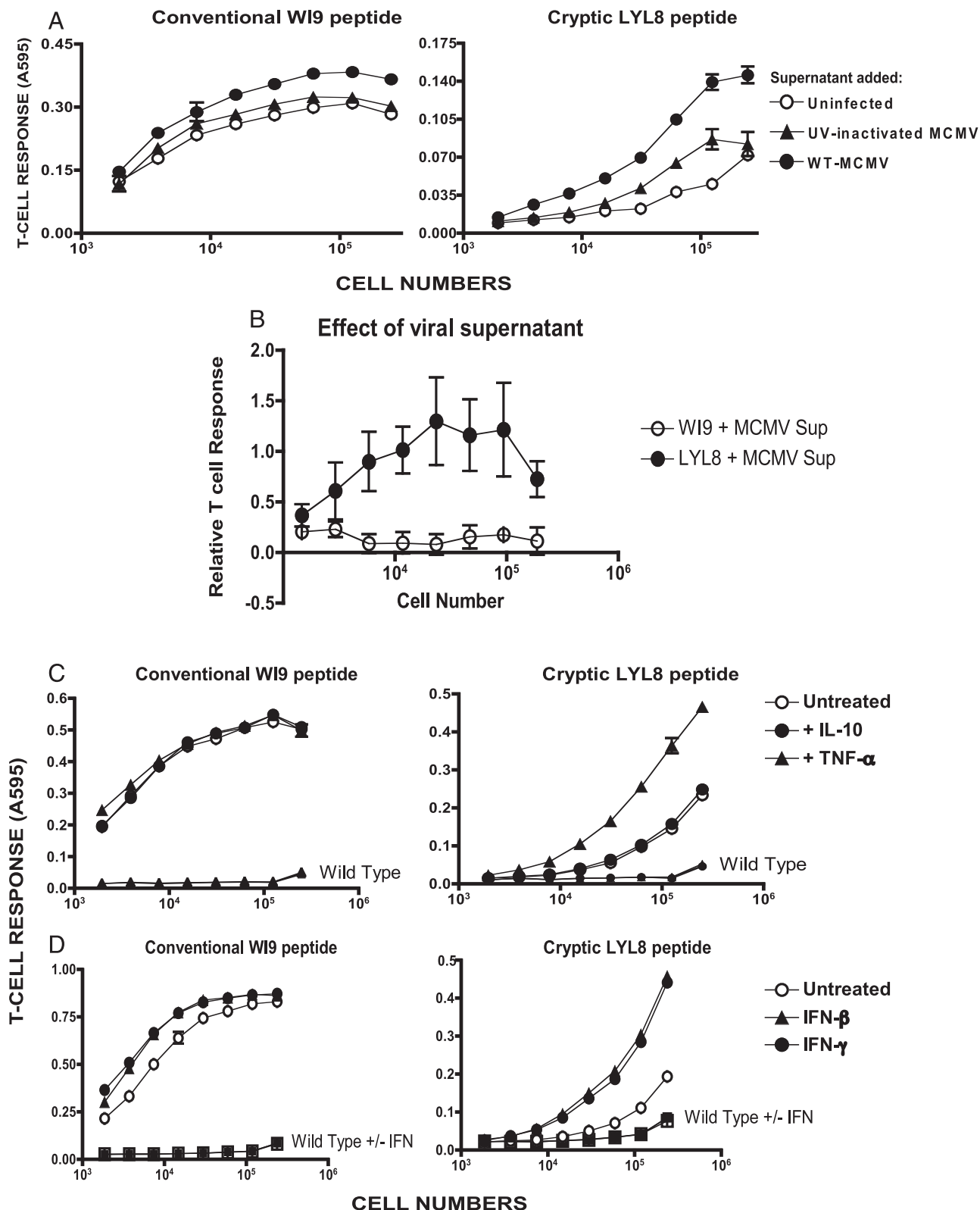


FIGURE 5. Enhancement of cryptic peptide presentation does not require direct virus infection. **(A)** Primary macrophages of the H-2^d haplotype were infected with wild-type MCMV-GFP or UV-inactivated MCMV-GFP for 6 h. Supernatant from the infected H-2^d macrophages was filtered with a 0.2- μ M filter and added to the WI9.LYL8 macrophages (H-2^b haplotype). The WI9.LYL8 macrophages were then harvested, and a T cell hybridoma assay was set up as described in Fig. 2. The y-axis indicates the T cell response (11p9Z-specific hybridoma response for the conventional peptide and the BCZ103-specific hybridoma response for the cryptic peptide), and x-axis indicates the cell numbers plated. Data are representative of three experiments. **(B)** T cell responses to the WI9 and LYL8 peptides were normalized to that of the uninfected samples for three distinct experiments. An unpaired *t* test (with Welch's correction) was performed, comparing the conventional and cryptic peptide responses: *p* < 0.05. **(C)** WI9.LYL8 primary macrophages were stimulated with TNF- α (0.1 μ g/ml) and IL-10 (0.1 μ g/ml). Cells were then harvested and a T cell hybridoma assay was set up as described in Fig. 2. The y-axis indicates the T cell response (11p9Z specific hybridoma response for the conventional peptide and the BCZ103-specific hybridoma response for the cryptic peptide), and x-axis indicates the cell numbers plated. Data are representative of two experiments. **(D)** WI9.LYL8 macrophages were (Figure legend continues)

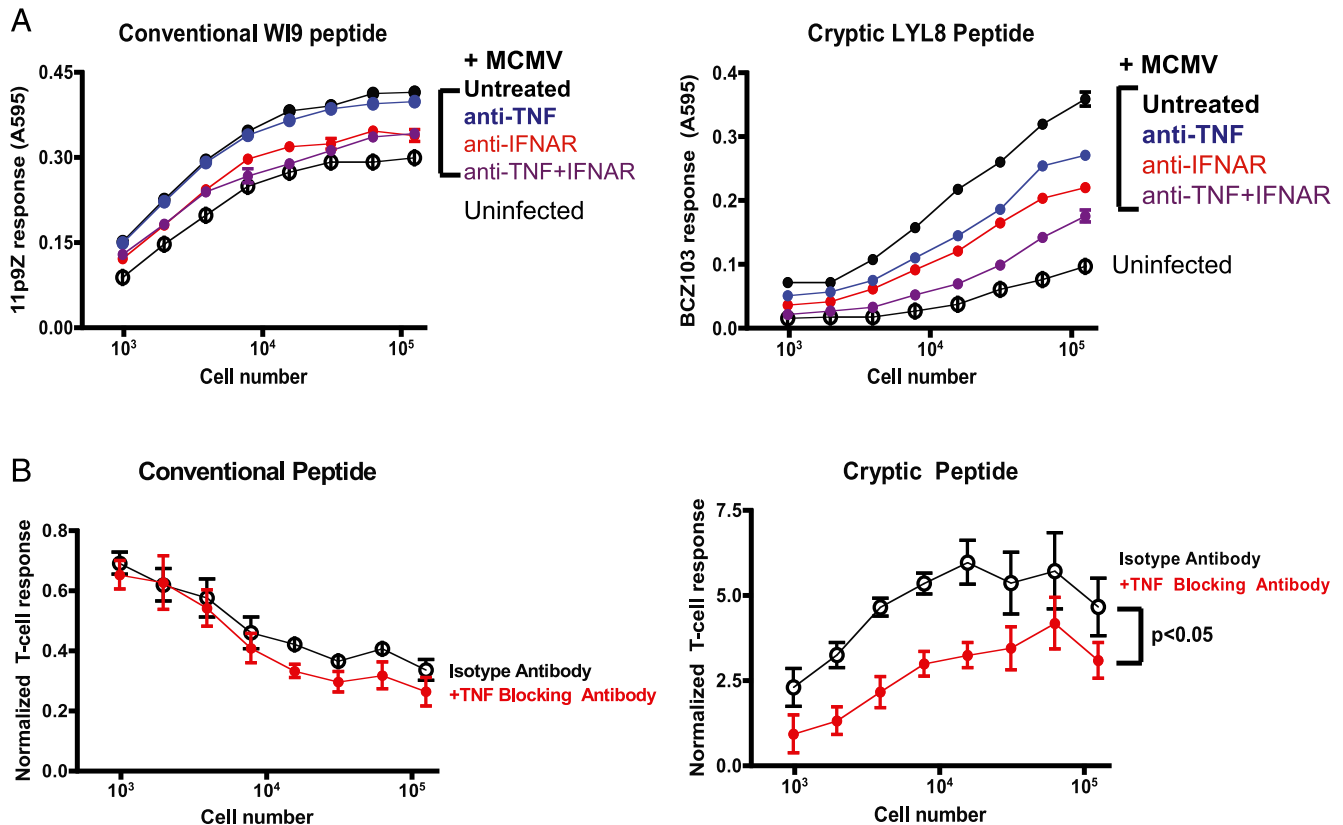


FIGURE 6. Blocking TNF and type I IFN signaling further inhibits the enhancement of cryptic peptide presentation upon MCMV infection. **(A)** WI9. LYL8 primary macrophages were infected with MCMV and then cultured with either TNF blocking Ab (MP6XT22), IFNAR 1 blocking Ab along with the respective isotype control Abs. Data are representative of two independent experiments with each experiment having a triplicate of samples for each condition. Cells were then harvested, and a T cell hybridoma assay was set up as described in Fig. 2. The y-axis indicates the T cell response (11p9Z-specific hybridoma response for the conventional peptide and the BCZ103-specific hybridoma response for the cryptic peptide), and x-axis indicates the cell numbers plated. **(B)** T cell response to infection and blocking Ab, from different experiments, were normalized to that of uninfected samples. The reciprocal of this value was taken and plotted as a percentage of the uninfected. Mann-Whitney *U* test showed a statistically significant effect of TNF blocking Ab on cryptic peptide presentation.

both the type I (IFN- β) and type II IFN (IFN- γ) by 8- and 5-fold, respectively, whereas conventional peptide presentation was increased only by 2-fold (Fig. 5D). Furthermore, T cell responses to the LYL8 peptide were significantly enhanced upon type I and type II IFN stimulation compared with the WI9 peptide (Supplemental Fig. 4D, 4E). Therefore, we have further shown that enhancement of cryptic peptide presentation does not require direct infection with virus; the enhancement can be caused by inflammatory cytokines.

To determine whether similar cytokines enhanced cryptic peptide presentation during MCMV infection, we used anti-TNF and anti-IFN receptor (IFNAR) to block the effect of these cytokines. A variety of different concentrations of this blocking Ab were tested. Primary WI9.LYL8 macrophages were infected with MCMV virus and cultured with TNF- α blocking Ab or IgG Isotype control Ab. When the TNF- α blocking Abs were used, enhancement of cryptic peptide presentation was inhibited. As measured by the relative T cell response, the enhancement with the TNF isotype Ab was 3-fold, whereas the enhancement with the TNF blocking Ab was just 2-fold. This suggested that there might be other inflammatory cytokines that could be acting to enhance cryptic peptide

presentation. To determine whether removal of IFN can diminish the enhanced cryptic peptide presentation phenomenon, IFNAR I blocking Abs were used at a concentration of 1.0 μ g/ml. WI9. LYL8 macrophages were infected with MCMV and cultured with isotype control (IgG) Abs or IFNAR I blocking Abs. As an additional control, infected cells were cultured with both TNF- α and IFNAR I blocking Abs (Fig. 6A). In the presence of IFNAR I blocking Abs, enhancement of cryptic peptide presentation was comparable to that with the isotype control Abs. Furthermore, in the presence of both TNF- α and IFNAR I blocking Abs, both cryptic and conventional peptide presentation were significantly diminished. This showed that both inflammatory cytokines play a role in causing enhanced cryptic peptide presentation. However, when the effect of TNF- α alone was examined, we found that TNF- α affected cryptic peptide presentation more than conventional peptide presentation. This was shown by quantifying the effect of the TNF- α blocking Abs. To quantify and combine different experiments, all the points on each curve, for the infected conditions, were normalized to its corresponding point on the uninfected curve. These values were then averaged across all the different experiments and plotted as a line graph (Fig. 6B). The

stimulated with type I or type II IFN. Cells were then harvested and a T cell hybridoma assay was set up as described in Fig. 2. The y-axis indicates the T cell response (11p9Z-specific hybridoma response for the conventional peptide and the BCZ103-specific hybridoma response for the cryptic peptide), and x-axis indicates the cell numbers plated. Data are representative of two experiments.

trend of each line indicates the effect of the condition. MCMV infection clearly enhances cryptic peptide presentation compared with uninfected cells, but conventional peptide presentation is diminished in comparison with uninfected cells. With the TNF- α blocking Ab treatment, there is a more significant inhibition of cryptic peptide presentation, compared with conventional peptide presentation.

Therefore, we have further shown that enhancement of cryptic peptide presentation does not require direct infection with virus; the enhancement can be caused by inflammatory cytokines. Using blocking Abs against inflammatory cytokines such as Type I IFN and TNF- α can diminish the enhancement of cryptic peptide presentation. However, TNF- α has a more significant effect on cryptic peptide presentation than the conventional peptide.

Discussion

Presentation of peptides generated by cryptic translation has emerged as an important source of antigenic precursors. In this study, we show that cryptic peptide presentation can be enhanced by physiological stimuli typically found in inflammatory milieu. Presentation of cryptic peptide was selectively enhanced when cells were stimulated with various TLR agonists or cells were infected with viruses such as MCMV or influenza. Remarkably, the enhanced cryptic peptide presentation could also be accomplished without direct virus infection by treating the cells with the inflammatory cytokines TNF or type I IFN. These findings clearly show that presentation of cryptic peptides is not simply a constitutive process but can also be regulated.

TLR stimulation induces a wide variety of transcriptional responses, relating to innate immunity, within the cell (30). Therefore, it is expected that TLRs would enhance global protein translation to induce immune response (31). This is indeed corroborated by our results with respect to TLR stimulation enhancing cryptic and conventional peptide presentation. Viral infection and cytokine treatments also enhanced presentation of cryptic peptides substantially more than conventionally translated peptides in APCs. This selective effect on cryptic versus conventional peptides is consistent with the distinct translational mechanisms that produce their antigenic precursors. Previous studies showed that initiation at the cryptic CUG codon was decoded as a leucine rather than the canonical methionine residue (12). Furthermore, the translational start at the CUG versus the canonical AUG codons was shown to be resistant to inhibitors of conventional translation (13, 21). Finally, a novel initiator tRNA was found that allowed translation initiation at CUG start codons (22). Because later stages of the Ag presentation pathway such as cytoplasmic proteolysis and TAP transport are unlikely to distinguish peptides arising from cryptic versus conventional translation, it is likely that selective regulation of cryptic peptide presentation occurs at an early stage, perhaps during polypeptide synthesis itself. This would suggest that a distinct factor(s) regulates the translation of peptides from CUG versus AUG start codons.

One possibility is a factor that is involved in cellular stress responses. TLRs have been implicated in regulating different cellular stress responses relating to endoplasmic reticulum stress and the unfolded protein response (UPR) (31). Furthermore, MCMV has also been shown to prevent the inhibition of global protein translation by regulating the UPR (32). Studying factors involved in the UPR and identifying whether they are linked to the differential CUG-initiated translation mechanism would help establish a mechanism for TLRs and MCMV enhancing cryptic peptide presentation.

Another possibility is to identify factors that are downstream of the TNF and IFN signaling pathways. One such factor is the p38

MAPK pathway, which can also be induced by different kinds of cellular stresses, osmotic shock, heat, and proinflammatory cytokines (33). Moreover, p38 MAPK is an important downstream effector of all TLR signaling pathways (34, 35), and inhibition of p38 MAPK signaling has been shown to cause distinct inflammatory responses (36, 37). Therefore, studying the p38 MAPK pathway and its downstream effectors could help identify a potential mechanism for regulation of cryptic peptide presentation.

One possible downstream effector could be one that is involved with the translation initiation pathway. For example, previous studies on the regulation of Met-initiator tRNA (Met-tRNA^{Met}) binding to the eIF2 complex have shown that this binding determines the efficiency of translation initiation (38). The AIMP3/p18 protein is anchored to the methionyl tRNA synthetase complex. AIMP3 knockdown resulted in reduced delivery of Met-initiator tRNA to eIF2 and inhibition of protein synthesis. The AIMP3 is found in a complex with AIMP1 and AIMP2 proteins and is known to mediate TNF signaling and activate macrophages through the p38 MAPK pathway (39). The AIMP2/p38 complex is also important for the assembly of the tRNA synthetase complex and has been shown to be an important regulator in response to genotoxic stresses (40). Given the localization of these AIMP proteins within the tRNA synthetase complex and their diverse functionality, it would be of interest to test the expression of these AIMP proteins in the context of MCMV infection and treatment with inflammatory cytokines to determine whether they can also regulate cryptic translation of antigenic precursors.

Regardless of the underlying mechanism, our findings imply that it may be possible to exploit enhanced cryptic peptide presentation for vaccines against viruses and even cancer cells. Viruses have been known to inhibit conventional Ag presentation and therefore it would be interesting to determine whether cryptic peptides, which are clearly enhanced upon viral infection, could be used to develop more effective vaccines. Likewise, enhanced cryptic peptide presentation could also be applicable to the cancer microenvironment that is rife with inflammatory cytokines like TNF and IFNs. If cryptic peptides are also enhanced in tumor cells, they could be used to develop effective peptide-based vaccines against cancer cells as well.

Acknowledgments

We thank Federico Gonzalez for support and David King for peptide synthesis.

Disclosures

The authors have no financial conflicts of interest.

References

- Blum, J. S., P. A. Wearsch, and P. Cresswell. 2013. Pathways of antigen processing. *Annu. Rev. Immunol.* 31: 443–473.
- Neefjes, J., M. L. Jongsma, P. Paul, and O. Bakke. 2011. Towards a systems understanding of MHC class I and MHC class II antigen presentation. *Nat. Rev. Immunol.* 11: 823–836.
- Shastri, N., S. Schwab, and T. Serwold. 2002. Producing nature's gene-chips: the generation of peptides for display by MHC class I molecules. *Annu. Rev. Immunol.* 20: 463–493.
- Yewdell, J. W., and C. V. Nicchitta. 2006. The DRiP hypothesis decennial: support, controversy, refinement and extension. *Trends Immunol.* 27: 368–373.
- Farfán-Arribas, D. J., L. J. Stern, and K. L. Rock. 2012. Using intein catalysis to probe the origin of major histocompatibility complex class I-presented peptides. *Proc. Natl. Acad. Sci. USA* 109: 16998–17003.
- Yewdell, J. W. 2011. DRiPs solidify: progress in understanding endogenous MHC class I antigen processing. *Trends Immunol.* 32: 548–558.
- Malarikannan, S., M. Afkarian, and N. Shastri. 1995. A rare cryptic translation product is presented by Kb major histocompatibility complex class I molecule to alloreactive T cells. *J. Exp. Med.* 182: 1739–1750.
- Cardinaud, S., A. Moris, M. Février, P. S. Rohrlisch, L. Weiss, P. Langlade-Demoyen, F. A. Lemonnier, O. Schwartz, and A. Habel. 2004. Identification of cryptic MHC I-restricted epitopes encoded by HIV-1 alternative reading frames. *J. Exp. Med.* 199: 1053–1063.

9. Goodenough, E., T. M. Robinson, M. B. Zook, K. M. Flanigan, J. F. Atkins, M. T. Howard, and L. C. Eisenlohr. 2014. Cryptic MHC class I-binding peptides are revealed by aminoglycoside-induced stop codon read-through into the 3' UTR. *Proc. Natl. Acad. Sci. USA* 111: 5670–5675.
10. Garbe, Y., C. Maletzki, and M. Linnebacher. 2011. An MSI tumor specific frameshift mutation in a coding microsatellite of MSH3 encodes for HLA-A0201-restricted CD8⁺ cytotoxic T cell epitopes. *PLoS One* 6: e26517.
11. Zook, M. B., M. T. Howard, G. Sinnathamby, J. F. Atkins, and L. C. Eisenlohr. 2006. Epitopes derived by incidental translational frameshifting give rise to a protective CTL response. *J. Immunol.* 176: 6928–6934.
12. Malarkannan, S., T. Hornig, P. P. Shih, S. Schwab, and N. Shastri. 1999. Presentation of out-of-frame peptide/MHC class I complexes by a novel translation initiation mechanism. *Immunity* 10: 681–690.
13. Schwab, S. R., J. A. Shugart, T. Hornig, S. Malarkannan, and N. Shastri. 2004. Unanticipated antigens: translation initiation at CUG with leucine. *PLoS Biol.* 2: e366.
14. Starck, S. R., and N. Shastri. 2011. Non-conventional sources of peptides presented by MHC class I. *Cell. Mol. Life Sci.* 68: 1471–1479.
15. Cardinaud, S., G. Consiglieri, R. Bouziat, A. Urrutia, S. Graff-Dubois, S. Fourati, I. Malet, J. Guernon, A. Guihot, C. Katlama, et al. 2011. CTL escape mediated by proteasomal destruction of an HIV-1 cryptic epitope. *PLoS Pathog.* 7: e1002049.
16. Rutkowski, M. R., O. Ho, and W. R. Green. 2009. Defining the mechanism(s) of protection by cytolytic CD8 T cells against a cryptic epitope derived from a retroviral alternative reading frame. *Virology* 390: 228–238.
17. Garrison, K. E., S. Champiat, V. A. York, A. T. Agrawal, E. G. Kallas, J. N. Martin, F. M. Hecht, S. G. Deeks, and D. F. Nixon. 2009. Transcriptional errors in human immunodeficiency virus type 1 generate targets for T-cell responses. *Clin. Vaccine Immunol.* 16: 1369–1371.
18. Li, C., K. Goudy, M. Hirsch, A. Asokan, Y. Fan, J. Alexander, J. Sun, P. Monahan, D. Seiber, J. Sidney, et al. 2009. Cellular immune response to cryptic epitopes during therapeutic gene transfer. *Proc. Natl. Acad. Sci. USA* 106: 10770–10774.
19. Andersen, R. S., S. R. Andersen, M. D. Hjortsø, R. Lyngaa, M. Idorn, T. M. Kølsgård, O. Met, P. Thor Straten, and S. R. Hadrup. 2013. High frequency of T cells specific for cryptic epitopes in melanoma patients. *Oncolimmunology* 2: e25374.
20. Weinzierl, A. O., D. Maurer, F. Altenberend, N. Schneiderhan-Marra, K. Klingel, O. Schoor, D. Wernet, T. Joos, H. G. Rammensee, and S. Stevanović. 2008. A cryptic vascular endothelial growth factor T-cell epitope: identification and characterization by mass spectrometry and T-cell assays. *Cancer Res.* 68: 2447–2454.
21. Schwab, S. R., K. C. Li, C. Kang, and N. Shastri. 2003. Constitutive display of cryptic translation products by MHC class I molecules. *Science* 301: 1367–1371.
22. Starck, S. R., V. Jiang, M. Pavon-Eternod, S. Prasad, B. McCarthy, T. Pan, and N. Shastri. 2012. Leucine-tRNA initiates at CUG start codons for protein synthesis and presentation by MHC class I. *Science* 336: 1719–1723.
23. Starck, S. R., Y. Ow, V. Jiang, M. Tokuyama, M. Rivera, X. Qi, R. W. Roberts, and N. Shastri. 2008. A distinct translation initiation mechanism generates cryptic peptides for immune surveillance. *PLoS One* 3: e3460.
24. Karttunen, J., S. Sanderson, and N. Shastri. 1992. Detection of rare antigen-presenting cells by the lacZ T-cell activation assay suggests an expression cloning strategy for T-cell antigens. *Proc. Natl. Acad. Sci. USA* 89: 6020–6024.
25. Malarkannan, S., P. P. Shih, P. A. Eden, T. Hornig, A. R. Zuberi, G. Christianson, D. Roopenian, and N. Shastri. 1998. The molecular and functional characterization of a dominant minor H antigen, H60. *J. Immunol.* 161: 3501–3509.
26. Serwold, T., S. Gaw, and N. Shastri. 2001. ER aminopeptidases generate a unique pool of peptides for MHC class I molecules. *Nat. Immunol.* 2: 644–651.
27. Mendoza, L. M., P. Paz, A. Zuberi, G. Christianson, D. Roopenian, and N. Shastri. 1997. Minors held by majors: the H13 minor histocompatibility locus defined as a peptide/MHC class I complex. *Immunity* 7: 461–472.
28. Aragón, T., S. de la Luna, I. Novoa, L. Carrasco, J. Ortín, and A. Nieto. 2000. Eukaryotic translation initiation factor 4G1 is a cellular target for NS1 protein, a translational activator of influenza virus. *Mol. Cell. Biol.* 20: 6259–6268.
29. Wang, X., and D. G. Chen. 2009. Recombinant murine cytomegalovirus vector activates human monocyte-derived dendritic cells in a NF- κ B-dependent pathway. *Mol. Immunol.* 46: 3462–3465.
30. Kawai, T., and S. Akira. 2010. The role of pattern-recognition receptors in innate immunity: update on Toll-like receptors. *Nat. Immunol.* 11: 373–384.
31. Cláudio, N., A. Dalet, E. Gatti, and P. Pierre. 2013. Mapping the crossroads of immune activation and cellular stress response pathways. *EMBO J.* 32: 1214–1224.
32. Qian, Z., B. Xuan, T. J. Chapa, N. Gualberto, and D. Yu. 2012. Murine cytomegalovirus targets transcription factor ATF4 to exploit the unfolded-protein response. *J. Virol.* 86: 6712–6723.
33. Katsoulidis, E., Y. Li, H. Mears, and L. C. Platanias. 2005. The p38 mitogen-activated protein kinase pathway in interferon signal transduction. *J. Interferon Cytokine Res.* 25: 749–756.
34. Dunne, A., and L. A. O'Neill. 2003. The interleukin-1 receptor/Toll-like receptor superfamily: signal transduction during inflammation and host defense. *Sci. STKE* 2003: re3.
35. O'Neill, L. A., and A. G. Bowie. 2007. The family of five: TIR-domain-containing adaptors in Toll-like receptor signalling. *Nat. Rev. Immunol.* 7: 353–364.
36. Bhattacharyya, S., D. E. Brown, J. A. Brewer, S. K. Vogt, and L. J. Muglia. 2007. Macrophage glucocorticoid receptors regulate Toll-like receptor 4-mediated inflammatory responses by selective inhibition of p38 MAP kinase. *Blood* 109: 4313–4319.
37. Jarnicki, A. G., H. Conroy, C. Brereton, G. Donnelly, D. Toomey, K. Walsh, C. Sweeney, O. Leavy, J. Fletcher, E. C. Lavelle, et al. 2008. Attenuating regulatory T cell induction by TLR agonists through inhibition of p38 MAPK signaling in dendritic cells enhances their efficacy as vaccine adjuvants and cancer immunotherapeutics. *J. Immunol.* 180: 3797–3806.
38. Kang, T., N. H. Kwon, J. Y. Lee, M. C. Park, E. Kang, H. H. Kim, T. J. Kang, and S. Kim. 2012. AIMP3/p18 controls translational initiation by mediating the delivery of charged initiator tRNA to initiation complex. *J. Mol. Biol.* 423: 475–481.
39. Park, S. G., E.-C. Choi, and S. Kim. 2010. Aminoacyl-tRNA synthetase-interacting multifunctional proteins (AIMPs): a triad for cellular homeostasis. *IUBMB Life* 62: 296–302.
40. Han, J. M., B. J. Park, S. G. Park, Y. S. Oh, S. J. Choi, S. W. Lee, S. K. Hwang, S. H. Chang, M. H. Cho, and S. Kim. 2008. AIMP2/p38, the scaffold for the multi-tRNA synthetase complex, responds to genotoxic stresses via p53. *Proc. Natl. Acad. Sci. USA* 105: 11206–11211.